

AD-A104 374

AIR FORCE GEOPHYSICS LAB HANSCOM AFB MA
A SIMPLIFIED PROCEDURE FOR DIRECT DETERMINATION OF REAL HEIGHT --ETC(U)

F/6 4/1

MAR 81 M M KLEIN
AFGL-TR-81-0070

UNCL ASSIFIED

NL

1 of 1
A
A-34374

END
DATE
FILED
40-81
DTIC

AD A104374

14 AFGL-TR-81-0070 AFGL-ERP-731
ENVIRONMENTAL RESEARCH PAPERS NO. 731

LEVEL



6 A Simplified Procedure for Direct Determination
of Real Height From Virtual Height Data

10 MILTON M. KLEIN

11 6 Mar 81

Approved for public release; distribution unlimited.

12 DTIC
13 ELECTED
14 SEP 18 1981
15 S H
16 2314
17 G6

SPACE PHYSICS DIVISION
AIR FORCE GEOPHYSICS LABORATORY
HANSOM AFB, MASSACHUSETTS 01731

PROJECT 2310

AIR FORCE SYSTEMS COMMAND, USAF

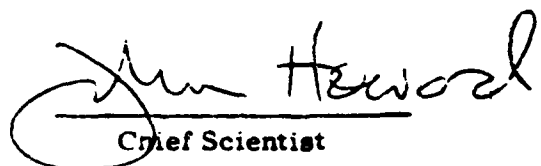


81 9 18 409578
35 065

This report has been reviewed by the ESD Information Office (OI) and is
releasable to the National Technical Information Service (NTIS).

This technical report has been reviewed and
is approved for publication.

FOR THE COMMANDER



Chief Scientist

Qualified requestors may obtain additional copies from the
Defense Technical Information Center. All others should apply to the
National Technical Information Service.

REPRODUCED BY UNTALED AGFA

AD-A104374



Unclassified

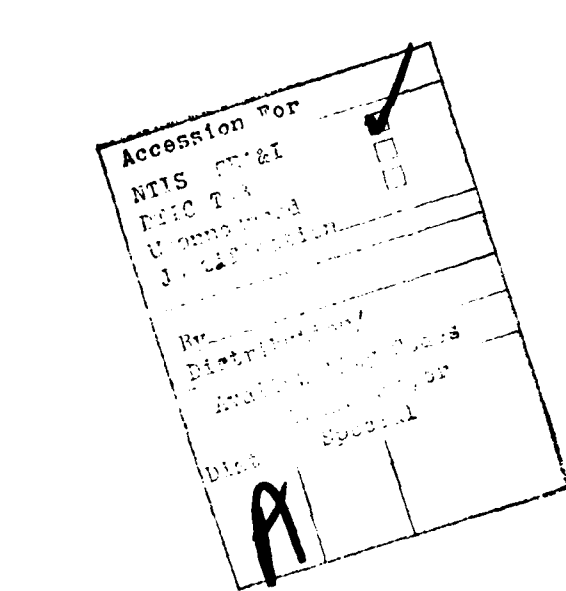
SECURITY CLASSIFICATION OF THIS PAGE (When Data Entered)

20. Abstract (Continued)

parabolic models of the ionosphere, and the corresponding real height values were then obtained by the present method. The results obtained showed that the calculated values of real height were in very good agreement with the exact values of real height.

To indicate the improvement obtainable with the introduction of additional parameters, a two-parameter function, which gives a somewhat more accurate representation of the dispersion curve than does the one-parameter function, was obtained for one case. However, the amount of computational labor required is considerably greater than that required for the present method.

In view of its simplicity and accuracy, it is felt that the one-parameter method is a useful analytic tool for determining real height from ionosonde data.



Unclassified

SECURITY CLASSIFICATION OF THIS PAGE (When Data Entered)

Contents

1. INTRODUCTION	5
2. DETERMINATION OF REAL HEIGHT	6
3. ANALYSIS FOR MODEL 1	11
4. ANALYSIS FOR MODEL 2	13
5. A METHOD FOR IMPROVING ACCURACY OF APPROXIMATE DISPERSION CURVE	18
6. RESULTS AND DISCUSSION	23
7. SUMMARY AND CONCLUSIONS	25

Illustrations

1. Variation of Parameter α With Frequency	8
2. Comparison of Exact and Approximate Dispersion Curves for Several Frequencies; $\theta = 10^\circ$, $f_H = 1.5$ MHz	9
3. Comparison of Exact and Approximate Dispersion Curves for Several Frequencies; $\theta = 30^\circ$, $f_H = 1.5$ MHz	10
4. Variation of Virtual Height $h'(f)$ With Frequency for the Two Parabolic Models	23
5. Comparison of Exact and Calculated Values of Real Height for the Two Parabolic Models	24

A Simplified Procedure for Direct Determination of Real Height From Virtual Height Data

I. INTRODUCTION

In a previous report¹ a method was presented for directly calculating real height from virtual height data obtained in the presence of a magnetic field. The method was based upon the representation of the non-linear portion of the dispersion relation between index of refraction and electron density by a simple power law, resulting in an Abel integral equation for the relation between real height and virtual height. The equation may then be solved explicitly for the real height as a function of frequency.

In making numerical applications, it was found that the use of different analytical forms for the two regions of the dispersion curve resulted in fairly tedious calculations. In addition, taking account of the variation of the several parameters with frequency (in particular the position separating the linear and non-linear portions of the curve) considerably enlarged the extent of the calculations. In seeking an alternative method, it was found that the entire dispersion curve could be represented with fairly good accuracy by a single power law, which greatly simplified and reduced the required numerical work.

(Received for publication 5 March 1981)

1. Klein, M. M. (1979) A Method for Direct Determination of Real Height From Virtual Height Data for the Auroral Region of the Ionosphere, AFGL-TR-79-0276, AD A083 139.

Two parabolic models were chosen for the investigation: In Model 1 the electron density increases to arbitrarily large values; in Model 2 the electron density reaches a maximum value. Model 1 was chosen because of the ease of making the required calculations; Model 2 was utilized because it has been applied frequently in studies of the ionosphere.

2. DETERMINATION OF REAL HEIGHT

The dispersion curve is written in the form

$$\mu^2 = (1 - X)^\alpha \quad (1)$$

where μ is the index of refraction and X is the ratio f_N^2/f^2 , where f_N is the plasma frequency and f is probing frequency. The exponent α is a parameter to be determined by fitting the curve given by Eq. (1) to the exact dispersion curve. The virtual height $h'(f)$, which is a function of input frequency f , is related to the real height h by the integral

$$h'(f) = \int_0^{h_r} \mu^1 dh \quad (2)$$

where h_r is the height of reflection, that is, when $\mu = 0$, and μ^1 is the group index of refraction and given by

$$\mu^1 = \frac{d}{df} (\mu f) \quad (3)$$

We may now write Eq. (2) in the form

$$\frac{d}{df} \int_0^{h_r} \mu f dh = h'(f) \quad (4)$$

in which, since μ vanishes at the upper limit h_r , we have taken the derivative outside the integral sign.

Integration of Eq. (4) yields

$$\int_0^{h_r} f(1-x)^{\alpha/2} dh = \int_0^f h'(f) df \quad (5)$$

which can be expressed in terms of f_N and f by

$$\int_0^{h_r} (f^2 - f_N^2)^{\alpha/2} f^{1-\alpha} dh = \int_0^f h'(f) df . \quad (6)$$

Since f is independent of real height, we may write Eq. (6) in the form

$$\int_0^{h_r} (f^2 - f_N^2)^{\alpha/2} dh = H'(f) \quad (7)$$

where

$$H'(f) = f^{\alpha-1} \int_0^f h'(f) df . \quad (8)$$

Changing to variables $F = f^2$, $\xi = f_N^2$, we can write Eq. (8) in the canonical form

$$\int_0^F (F - \xi)^{\alpha/2} u d\xi = H'(F) \quad (9)$$

where $u = \frac{dh}{dF}$. We may invert Eq. (9) by the Laplace transform technique to yield (see Ref. 1 for details)

$$h = \frac{\sin \pi \alpha/2}{\pi \alpha/2} \int_0^{F_v} \frac{dF}{(F_v - F)^{\alpha/2}} \frac{dH'(F)}{dF} \quad (10)$$

or

$$h = \frac{\sin \pi \alpha/2}{\pi \alpha/2} \int_0^{f_v} \frac{df}{(f_v^2 - f^2)^{\alpha/2}} \frac{dH'(f)}{df} \quad (11)$$

where F_v or f_v is the maximum value of F or f corresponding to the reflection height.

To determine the value of α , the approximate dispersion curve was compared with the exact curve for several values of α . In general, the approximate curve was above the exact curve for small values of X and below at the larger values. A value of α was chosen that was estimated to give the least overall error. A plot of α as a function of frequency is given in Figure 1 for two values of θ , where θ is the angle between the ray and the magnetic field. A comparison of the exact and approximate dispersion curves is given in Figures 2 and 3 for the same two angles. The exact curve was computed for several values of the gyromagnetic frequency $Y = f_H/f$ at $f_H = 1.5$ MHz. It is noted that the curves are generally in good agreement at an angle of 30° , while at 10° the agreement is not as good, particularly at

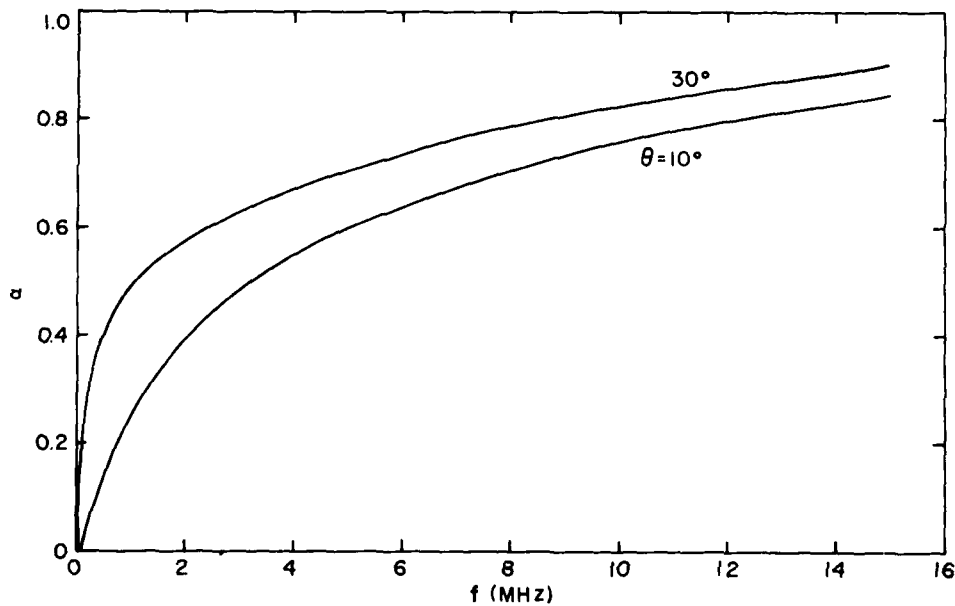


Figure 1. Variation of Parameter α With Frequency

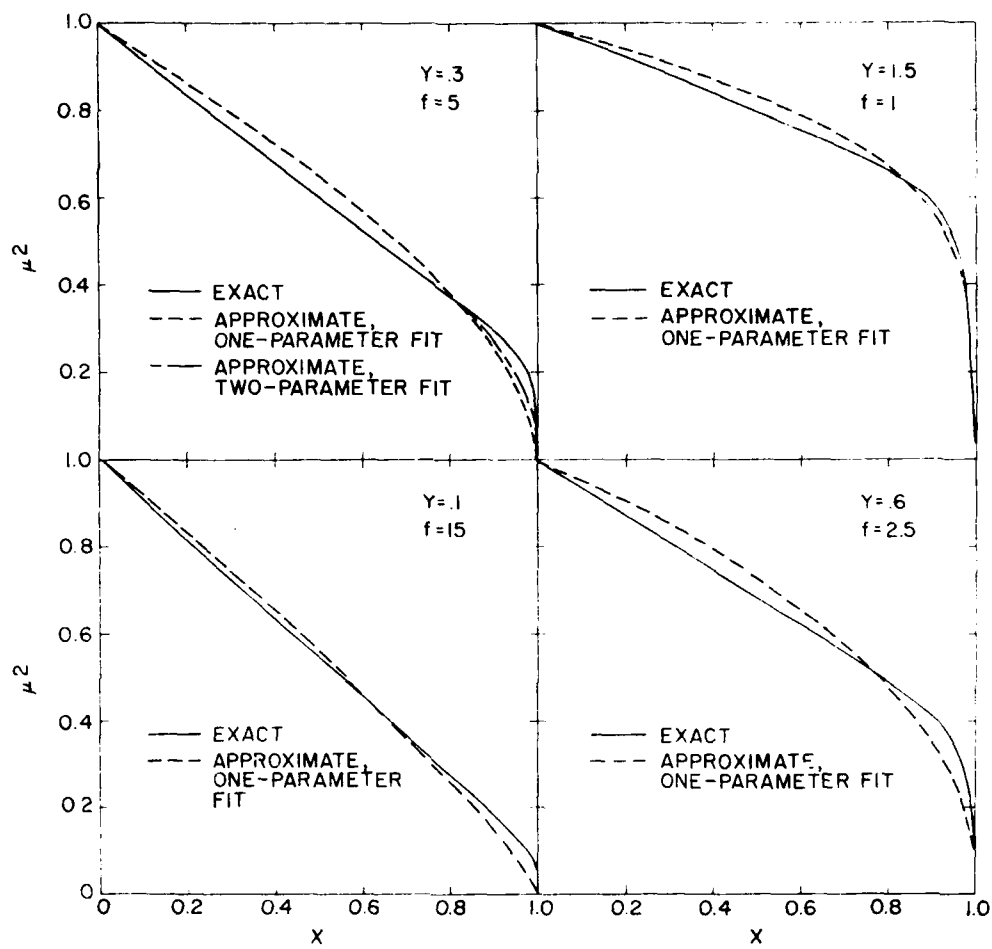


Figure 2. Comparison of Exact and Approximate Dispersion Curves for Several Frequencies; $\theta = 10^{\circ}$; $f_{11} = 1.5$ MHz

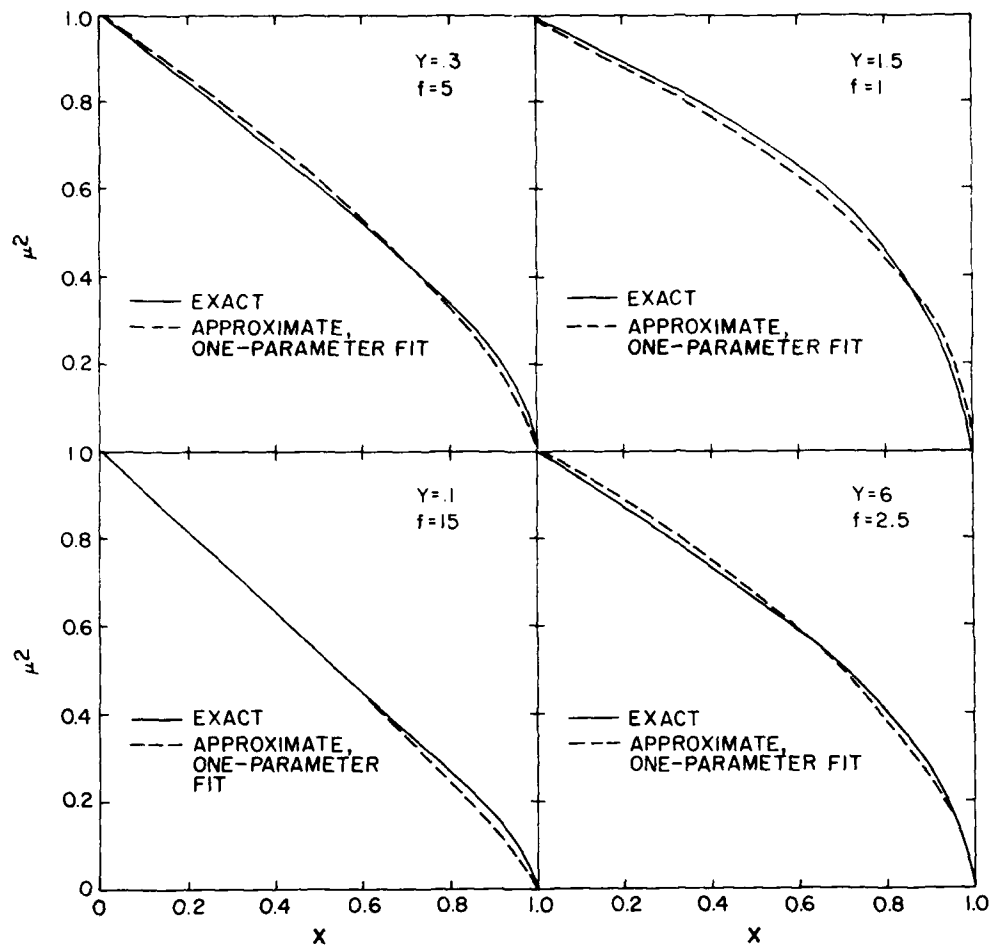


Figure 3. Comparison of Exact and Approximate Dispersion Curves for Several Frequencies; $\theta = 30^\circ$, $f_H = 1.5$ MHz

the lower frequencies. However, since the error changes sign as X goes to larger values, it is anticipated that the calculated values of real height for 10° should not differ much from those for 30° .

3. ANALYSIS FOR MODEL I

The electron density N is given by

$$\frac{N}{N_p} = \frac{f^2}{f_p^2} e^{(h - h_0)^{1/2}} \quad (12)$$

where h_0 is a reference height at which N vanishes, f_p is the maximum plasma frequency corresponding to the maximum probing frequency, and e is a constant determined by the value of N at some particular height. In this model, the slope is horizontal at h_0 and N increases to arbitrarily large values.

The virtual height is, from Eq. (4), given by

$$h'(f) = \frac{d}{df} (fI) \quad (13)$$

where

$$I = \int_0^1 (1 - X)^{\sigma/2} dh \quad (14)$$

Using Eq. (12), we can write I in the form

$$I = 2 \frac{b^4}{c^2} \int_0^1 (1 - X)^{\sigma/2} dX \quad (15)$$

where $b = f/f_p$, with f_p the plasma frequency corresponding to the maximum electron density N_p . Integration of Eq. (15) yields

$$I = 2 \frac{b^4}{c^2} \frac{1}{1 + \sigma/2} \frac{1}{2 + \sigma/2} \quad (16)$$

The virtual height $h'(f)$ is then, from Eq. (13),

$$h'(f) = \frac{d}{df} \left(2f \frac{b^4}{c^2} \frac{1}{1 + \sigma/2} \frac{1}{2 + \sigma/2} \right) \quad (17)$$

which yields

$$h^*(f) = 10 \frac{b^4}{c^2} \frac{1}{1+\alpha/2} \frac{1}{2+\alpha/2} + f \frac{b^4}{c^2} \frac{d\alpha}{df} \frac{3+\alpha}{(1+\alpha/2)^2 (2+\alpha/2)^2} . \quad (18)$$

An examination of the second term shows that, because of the small value of $\frac{d\alpha}{df}$ (see Figure 1), it is typically only a few percent of the first term. We shall therefore, for simplicity, neglect this term.

Using Eq. (7), the quantity $\frac{dH^*(f)}{df}$ is given by

$$\frac{dH^*(f)}{df} = \frac{d}{df} \left(f^{\alpha-1} \int_0^f h^*(f) df \right) \quad (19)$$

which yields

$$\frac{dH^*(f)}{df} = A f^{3+\alpha} \quad (20)$$

$$A = \frac{10}{1+\alpha/2} \frac{1}{2+\alpha/2} \frac{1}{f_p^4 c^2} \quad (21)$$

in which, in view of the small value of $\alpha = 1$, we have ignored variation in $f^{\alpha-1}$ and have again neglected terms in $\frac{d\alpha}{df}$.

The real height, Eq. (10), now takes the form

$$h = \frac{\sin \pi \alpha/2}{\pi \alpha/2} A \int_0^{f_V} \frac{f^{3+\alpha}}{(f_V^2 - f^2)^{\alpha/2}} df \quad (22)$$

which can be expressed in terms of a new variable, $u = f/f_V$, as

$$h = \frac{\sin \pi \alpha/2}{\pi \alpha/2} A f_V^4 \int_0^1 \frac{u^{3+\alpha}}{(1-u^2)^{\alpha/2}} du . \quad (23)$$

The integral in Eq. (23) can be expressed in terms of the Gamma function and Eq. (23) written as

$$h = \frac{\sin \pi \alpha/2}{\pi \alpha/2} \frac{A f_V^4}{4} \Gamma(1-\alpha/2) \Gamma(2+\alpha/2) . \quad (24)$$

4. ANALYSIS FOR MODEL 2

Here the electron density is specified by

$$\frac{N}{N_p} = \frac{r_p^2}{r^2} = 1 - \xi^2 \quad (25)$$

$$\xi = \frac{h_m - h}{a} \quad (26)$$

where h_m is the height corresponding to the maximum electron density and a is a constant determined by the value of N at some particular height. The virtual height is then given by

$$h'(f) = \frac{d}{df} (fJ) \quad (27)$$

$$J = \frac{ab^2}{2} \int_0^1 \frac{(1-x)^{\alpha/2}}{(1-b^2 x)^{1/2}} dx . \quad (28)$$

The integral J cannot be evaluated exactly for arbitrary b . For values of b less than one a power series solution may be obtained, while for b close to one a combined numerical and analytical technique may be utilized.

For b less than one, the quantity $(1-b^2 x)^{-1/2}$ can be expanded into a power series and the integral J in Eq. (28) takes the form

$$J = \frac{ab^2}{2} \left(J_0 + \frac{1}{2} b^2 J_1 + \frac{3}{8} b^4 J_2 + \frac{5}{16} b^6 J_3 + \frac{35}{128} b^8 J_4 + \dots \right) \quad (29)$$

where

$$J_n = \int_0^1 (1-x)^{\alpha/2} x^n dx , \quad n = 0, 1, 2, \dots$$

The integral J_n can be evaluated by successive integration by parts, or by expressing J_n in terms of the Beta function

$$B(m, n) = \int_0^1 x^{m-1} (1-x)^{n-1} dx$$

$$= \frac{\Gamma(m)\Gamma(n)}{\Gamma(m+n)} . \quad (30)$$

The integral J_n can then be written as

$$J_n = B\left(n+1, \frac{\alpha}{2} + 1\right)$$

$$= \frac{\Gamma(n+1)\Gamma\left(\frac{\alpha}{2} + 1\right)}{\Gamma(n+2+\alpha/2)} \quad (31)$$

which can be reduced to

$$J_n = \frac{1}{1+\alpha/2} \left(\frac{1}{2+\alpha/2} \frac{2}{3+\alpha/2} \cdots \frac{n}{n+1+\alpha/2} \right) \quad n = 1, 2, 3, \dots$$

$$J_0 = \frac{1}{1+\alpha/2} . \quad (32)$$

The virtual height $h'(f)$ is then given by

$$h'(f) = \frac{a}{2} \left(3b^2 J_0 + \frac{5}{2} b^4 J_1 + \frac{21}{8} b^6 J_2 + \frac{45}{16} b^8 J_3 + \frac{385}{128} b^{10} J_4 + \dots \right) . \quad (33)$$

Values of the virtual height can be obtained with good accuracy and with only a few terms for $b \leq 0.8$.

The real height is, using Eqs. (4) and (10), now given by

$$h = \frac{\sin \pi \alpha/2}{\pi \alpha/2} \frac{a}{2} \int_0^{f_v} \frac{f^{\alpha-1}}{(f_v^2 - f^2)^{\alpha/2}} h'(f) df \quad (34)$$

which may be expressed in the form

$$h = \frac{\sin \pi \alpha/2}{\pi \alpha/2} \frac{a}{2} \left(3J_0 K_0 + \frac{5}{2} J_1 K_1 + \frac{21}{8} J_2 K_2 + \frac{45}{16} J_3 K_3 + \frac{385}{128} J_4 K_4 + \dots \right) \quad (35)$$

where the typical term K_n is given by

$$K_n = b_v^{2n+2} \int_0^1 \frac{u^{2n+1+\alpha}}{(1-u^{2\alpha/2})} du , \quad n = 0, 1, 2, \dots , \quad (36)$$

$u = f/f_v$ and $b_v = f_v/f_p$. The integral K_n may be expressed in terms of Gamma functions by

$$K_n = b_v^{2n+2} \frac{\Gamma(1-\alpha/2)\Gamma(n+1+\alpha/2)}{2\Gamma(n+2)} . \quad (37)$$

For values of b close to unity, the integral J , Eq. (28), is written in the form

$$J = \frac{ab^2}{2} \int_0^1 (1-X)^{(\alpha-1)/2} \frac{(1-X)^{1/2}}{(1-b^2X)^{1/2}} dX . \quad (38)$$

Since $\frac{1-\alpha}{2}$ is small (~ 0.1), the quantity $(1-X)^{(\alpha-1)/2}$ is a slowly varying quantity and will be replaced by its average value. We then write Eq. (34) in the form

$$J = \frac{ab^2}{2} g \int_0^1 \frac{(1-X)^{1/2}}{(1-b^2X)^{1/2}} dX \quad (39)$$

where g is the average value of $(1-X)^{(1-\alpha)/2}$ and given by

$$g = \int_0^1 (1-X)^{(\alpha-1)/2} dX = \frac{2}{\alpha+1} . \quad (40)$$

The integral in Eq. (39) can now easily be evaluated to yield

$$J = \frac{ab^2}{2} g \left[\frac{1}{b^2} - \frac{1}{2} \frac{(1-b^2)}{b^3} \ln \left(\frac{1+b}{1-b} \right) \right] \quad (41)$$

and the virtual height, Eq. (27), takes the form

$$h'(f) = \frac{agb}{2} \ln \left(\frac{1+b}{1-b} \right) . \quad (42)$$

To check the accuracy of the g term, the value J given by Eq. (41) was compared with that given by Eq. (29) for b in the range 0.7 to 0.85; agreement to within a few percent was obtained. The quantity $\frac{dH'(f)}{df}$ is, using Eq. (19), now given by

$$\frac{dH'(f)}{df} = \frac{agb}{2} f^{\alpha-1} \ln \left(\frac{1+b}{1-b} \right) \quad (43)$$

and the real height h is now calculated from

$$h = \frac{\sin \pi \alpha/2}{\pi \alpha/2} \frac{ag}{2} \int_0^{f_v} f^{\alpha-1} b \ln \left(\frac{1+b}{1-b} \right) \frac{df}{(f_v^2 - f^2)^{\alpha/2}} \quad (44)$$

which can be written in the form

$$h = \frac{\sin \pi \alpha/2}{2\alpha/2} \frac{ag}{2} b_v \int_0^1 u^\alpha \ln \left(\frac{1+b_v u}{1-b_v u} \right) \frac{du}{(1-u^2)^{\alpha/2}} \quad (45)$$

where

$$u = f/f_v$$

The integral in Eq. (40) can be evaluated by expansion of the logarithmic term as a power series in $b_v u$. However, this series expansion offers no advantage over the series expansion in powers of b , Eq. (29), a large number of terms being required for b_v close to unity in either case. Since the integral can be evaluated exactly in the neighborhood of the singularity ($b_v = 1$), we have utilized numerical integration over about 95 percent of the range, and evaluated the remaining 5 percent analytically. We write the integral L in Eq. (45) as

$$L = L_1 + L_2 \quad (46)$$

where

$$L_1 = \int_0^1 u^\alpha \ln \left(\frac{1+b_v u}{1-b_v u} \right) \frac{du}{(1-u^2)^{\alpha/2}} \quad (47)$$

$$I_2 = \int_{u_1}^1 u^\alpha \ln \left(\frac{1 + b_v u}{1 - b_v u} \right) \frac{du}{(1 - u^2)^{\alpha/2}} \quad (48)$$

and u_1 , the point separating I_1 and I_2 , is about 0.95. The integral I_1 was evaluated numerically by Simpson's rule. To evaluate I_2 , we change the variable to $\epsilon = 1 - u$, $\epsilon_1 = 1 - u_1$, and obtain

$$I_2 = \frac{1}{2^{\alpha/2}} (M_1 - M_2 - M_3) \quad (49)$$

where

$$M_1 = \ln(1 + b_v) \frac{\epsilon_1^{1-\alpha/2}}{1 - \alpha/2} \quad (50)$$

$$M_2 = \frac{b_v}{1 + b_v} \frac{\epsilon_1^{2-\alpha/2}}{2 - \alpha/2} \quad (51)$$

$$M_3 = \int_0^{\epsilon_1} \frac{\ln(1 - b_v + b_v \epsilon)}{\epsilon^{\alpha/2}} d\epsilon \quad (52)$$

For $b_v = 1$, M_3 becomes

$$M_3 = \int_0^{\epsilon_1} \frac{\ln \epsilon}{\epsilon^{\alpha/2}} d\epsilon = \frac{\epsilon_1^{1-\alpha/2}}{1 - \alpha/2} \left(\ln \epsilon_1 - \frac{1}{1 - \alpha/2} \right) \quad (53)$$

For $b_v \neq 1$, M_3 cannot be expressed in terms of elementary functions, but can be expressed in terms of the digamma function.² Integration by parts yields for M_3

$$M_3 = \frac{\ln(1 - b_v + b_v \epsilon_1)}{1 - \alpha/2} \epsilon_1^{1-\alpha/2} - \frac{b}{1 - \alpha/2} M_4 \quad (53a)$$

2. Abramowitz, M., and Stegun, I., Editors (1964) Handbook of Mathematical Functions, National Bureau of Standards, AMS 55, Washington, D.C., Chap. 6.

$$M_4 = \frac{\epsilon^{2-\alpha/2}}{1-b_V} \int_0^1 \frac{t^{1-\alpha/2}}{1 + \frac{b_V \epsilon_1 t}{1-b_V}} dt = \frac{\epsilon^{2-\alpha/2}}{1-b_V} \int_0^1 \frac{t^{1-\alpha/2}}{1+t - t \left(1 - \frac{b_V \epsilon_1}{1-b_V}\right)} dt \quad (54)$$

where $t < \epsilon/\epsilon_1$. We may now approximate M_4 by

$$M_4 = \frac{\epsilon^{2-\alpha/2}}{1-b_V} \left[\int_0^1 \frac{t^{1-\alpha/2}}{1+t} dt + \left(1 - \frac{b_V \epsilon_1}{1-b_V}\right) \int_0^1 \frac{t^{2-\alpha/2}}{(1+t)^2} dt \right] \quad (55)$$

where the integrals in Eq. (55) are given by³

$$\int_0^1 \frac{t^{k-1}}{t+1} dt = \frac{1}{2} \left[\psi \left(\frac{k+1}{2} \right) - \psi \left(\frac{k}{2} \right) \right], \quad k > 0 \quad (56)$$

$$\int_0^1 \frac{t^{k-1}}{(t+1)^2} dt = \frac{1}{2} - \frac{k-1}{2} \left[\psi \left(\frac{k+1}{2} \right) - \psi \left(\frac{k}{2} \right) \right], \quad k > 0 \quad (57)$$

and $\psi(z)$ is the digamma function

$$\psi(z) = \frac{d}{dz} \ln \Gamma(z). \quad (58)$$

5. A METHOD FOR IMPROVING ACCURACY OF APPROXIMATE DISPERSION CURVE

As indicated in Section 2, the accuracy of the calculated values of real height depends to a large extent upon how well the dispersion curve can be represented by a single parameter function such as the form given by Eq. (1). The results obtained, as shown by Figure 2, indicated good accuracy at 30° , the accuracy being only fair in the neighborhood of 10° . An increase in accuracy can be achieved by introducing additional parameters, the significant practical restriction being the

3. Gröbner, W., and Hofreiter, N. (1965) Integraltafel, Zweiter Teil, Bestimmte Integrale, Springer-Verlag, Wien, New York, p. 176.

amount of computational labor introduced. Because of the non-linearity of the method, additional terms cannot be introduced in a straightforward manner. For example, in the two-parameter function

$$2\mu = (1 - X)^{\alpha_1/2} + (1 - X)^{\alpha_2/2} , \quad (59)$$

it is tedious to obtain α_1 and α_2 but, more significantly, a non-integral power of frequency is introduced into the electron density term in Eq. (4) that renders prohibitively difficult the inversion of the integral equation for real height. However, a form that does lead to a practical solution is the two-parameter function

$$\mu = (1 - X)^{\alpha/2} (1 - aX) \quad (60)$$

where α and a are parameters to be determined. Integration of Eq. (4) now takes the form

$$(F - \xi)^{\alpha/2} u d\xi - a \frac{\xi}{F} (F - \xi)^{\xi/2} = H'(F) \quad (61)$$

which can be written as

$$(1 - a) \int_0^F (F - \xi)^{\alpha/2} u d\xi + a \frac{1}{F} \int_0^F \frac{(F - \xi)^{1+\alpha/2}}{F} u d\xi = H'(F) . \quad (62)$$

The Laplace transform of Eq. (62) is

$$(1 - a) \Gamma(1 + \alpha/2) \frac{\bar{u}(s)}{s^{1+\alpha/2}} + a \Gamma\left(2 + \frac{\alpha}{2}\right) \int_s^\infty \frac{\bar{u}(s)}{s^{2+\alpha/2}} ds = \bar{H}(s) \quad (63)$$

which can be written as

$$\frac{d\bar{v}(s)}{ds} - \frac{a}{1 - a} \left(1 + \frac{\alpha}{2}\right) \frac{\bar{v}(s)}{s} = - \frac{1}{1 - a} \frac{1}{1 + \alpha/2} \frac{\bar{H}(s)}{s} \quad (64)$$

where

$$\bar{v}(s) = \int_s^\infty \frac{\bar{u}(s)}{s^{2+\alpha/2}} ds . \quad (65)$$

The solution of Eq. (64) is

$$\bar{v}(s) = cs^b \int_s^\infty s^{-1-b} \bar{H}(s) ds \quad (66)$$

where

$$b = \frac{a}{1-a} (1 + \alpha/2)$$

$$c = \frac{1}{1-a} \frac{1}{\Gamma(1 + \alpha/2)} .$$

Differentiation of Eq. (66) yields

$$\frac{d\bar{v}(s)}{ds} = -\frac{c}{s} \bar{H}(s) + cbs^{b-1} \int_s^\infty s^{b-1} \bar{H}(s) ds \quad (67)$$

which, in terms of $\bar{u}(s)$, takes the form

$$\bar{u}(s) = \frac{cs^2}{s^{1-\alpha/2}} \bar{H}(s) - cb \frac{s^2}{s^{1-b-\alpha/2}} \int_s^\infty \frac{\bar{H}(s)}{s^{1+b}} ds . \quad (68)$$

The inverse transform of Eq. (68) is then

$$\begin{aligned} dh &= \frac{c}{\Gamma(1 - \alpha/2)} \frac{d^2}{d\xi^2} \int_0^{F_v} \frac{H'(F)}{(F_v - F)^{\alpha/2}} - \frac{cb}{\Gamma(1 - b - \alpha/2)} \frac{d^2}{d\xi^2} \int_0^{F_v} \\ &\quad \frac{G(F)}{(F_v - F)^{b+\alpha/2}} dF \end{aligned} \quad (69)$$

where

$$G(F) = \frac{1}{\Gamma(1 - b)} \frac{1}{F} \int_0^F (F - t)^b H'(t) dt . \quad (70)$$

Integration of Eq. (69) and carrying through the remaining differentiation yields

$$h = \frac{c}{\Gamma(1 - \alpha/2)} \int_0^{F_v} \frac{1}{(F_v - F)^{\alpha/2}} \frac{dH'(F)}{dF} dF - \frac{cb}{\Gamma(1 - b - \alpha/2)} \int_0^{F_v} \frac{1}{(F_v - F)^{b+\alpha/2}} \frac{dG}{dF} dF \quad (71)$$

where $\frac{dG(F)}{dF}$ is given by

$$\frac{dG(F)}{dF} = -\frac{1}{\Gamma(1 - b)} \frac{1}{F^2} \int_0^F (F - t)^b H'(t) dt + \frac{b}{\Gamma(1 - b)} \int_0^F (F - t)^{b-1} H'(t) dt. \quad (72)$$

An approximate solution, somewhat simpler in form than Eq. (71), can be obtained if a is small compared to unity. Subsequent numerical calculations show that this is indeed the case. Neglecting the term in a in Eq. (63) and solving for $\bar{u}(s)$ in terms of $\bar{H}(s)$ yields

$$\bar{u}(s) = \frac{s^{1+\alpha/2}}{(1 - a)} \frac{1}{\Gamma(1 + \alpha/2)} \bar{H}(s), \quad (73)$$

which enables us to now write Eq. (63) in the form

$$\bar{u}(s) = \frac{1}{(1 - a)} \frac{1}{\Gamma(1 + \alpha/2)} \left[\frac{s^2}{s^{1-\alpha/2}} \bar{H}(s) - \frac{a(1 + \alpha/2)}{1 - a} \frac{s^2}{s^{1-\alpha/2}} \int_s^\infty \frac{\bar{H}(s)}{s} ds \right]. \quad (74)$$

Taking the inverse transform of Eq. (74) yields

$$\frac{dh}{d\xi} = \frac{\sin \pi \alpha/2}{(1 - a) \pi \alpha/2} \left[\frac{d^2}{d\xi^2} \int_0^{F_v} \frac{H'(F)}{(F_v - F)^{\alpha/2}} dF - \frac{a(1 + \alpha/2)}{(1 - a)} \frac{d^2}{d\xi^2} \int_0^{F_v} \frac{G(F)}{(F_v - F)^{\alpha/2}} dF \right] \quad (75)$$

where

$$G(F) = \frac{1}{F} \int_0^F H(t) dt . \quad (76)$$

Integrating and carrying through the remaining differentiation yields

$$h = \frac{\sin \pi \alpha/2}{\pi \alpha/2} \left[\frac{1}{1-a} \int_0^{F_v} \frac{H(F)}{(F_v - F)^{\alpha/2}} dF - \frac{a(1+\alpha/2)}{(1-a)^2} \int_0^{F_v} \frac{1}{(F_v - F)^{\alpha/2}} \frac{dG(F)}{dF} dF \right] \quad (77)$$

where

$$\frac{dG(F)}{dF} = -\frac{1}{F^2} \int_0^F H(t) dt + \frac{1}{F} H(F) . \quad (78)$$

To show the improvement in the approximation to the dispersion curve, the case $\theta = 10^\circ$, $f = 5$ was studied numerically. The parameters α and a were determined by fitting the approximate curve, Eq. (60), to the exact dispersion curve at the points X_1 and X_2 , setting

$$\mu_1 = (1 - X_1)^{\alpha/2} (1 - a X_1)$$

$$\mu_2 = (1 - X_2)^{\alpha/2} (1 - a X_2)$$

where

$$X_1 = 0.3 , \quad \mu_1 = 0.872$$

$$X_2 = 0.7 , \quad \mu_2 = 0.671 .$$

Elimination of α from these equations yields

$$\frac{\ln \mu_1}{\ln \mu_2} = \frac{\ln (1 - X_1)}{\ln (1 - X_2)} = 0.296 \quad (79)$$

where

$$q = \frac{\mu}{1 - aX_1} .$$

A solution to Eq. (79) was obtained graphically, yielding $a = 0.21$; the value of α was then determined as 0.40 . A check of the approximate dispersion curve against the exact curve, Figure 3, now shows excellent agreement up to $x = 0.8$; for $X > 0.8$ the improvement is only fair. It is likely that a better approximation for X can be obtained by choosing a larger value for X_2 , say $X_2 = 0.8$ or 0.9 .

6. RESULTS AND DISCUSSION

The calculated values for virtual height as a function of frequency are presented in Figure 4, and those for the real height are shown in Figure 5. The virtual and real height have been normalized to the maximum real height. The effect of the angle θ between the ray and the magnetic field was very small and, consequently, only a single curve has been used to represent an angle of 10° or 30° . The virtual

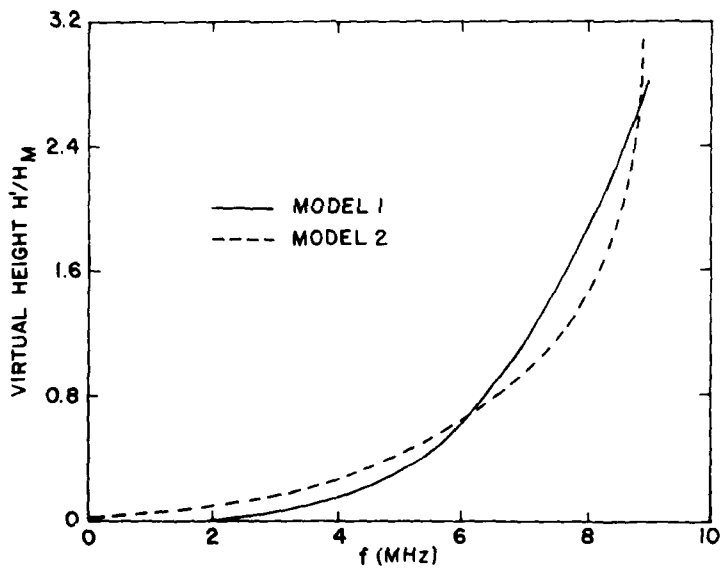


Figure 4. Variation of Virtual Height $h'(f)$ With Frequency for the Two Parabolic Models (the virtual height has been normalized to maximum real height)

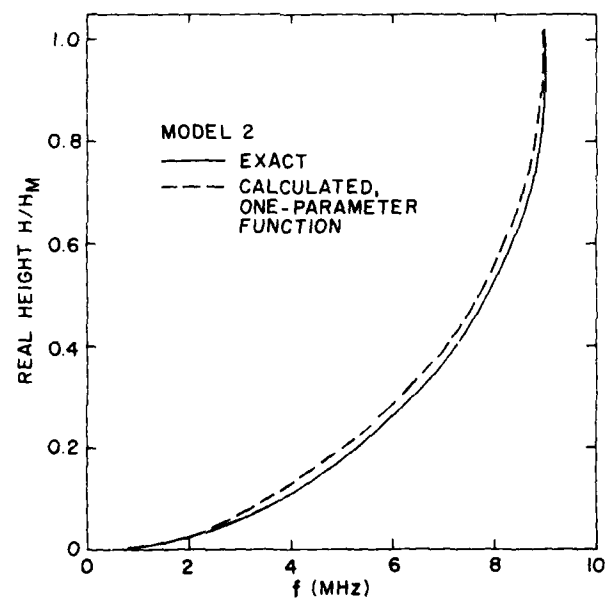
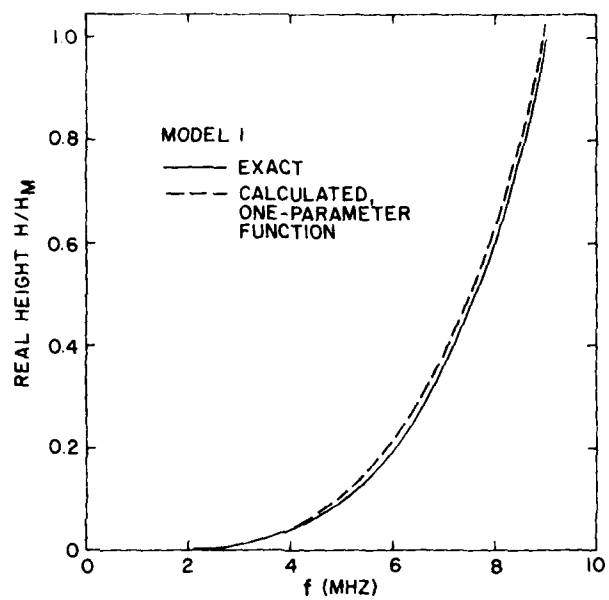


Figure 5. Comparison of Exact and Calculated Values of Real Height for the Two Parabolic Models (the real height has been normalized to maximum real height)

height for Model 2 initially rises more rapidly than that for Model 1, then lags behind until near the maximum frequency where it increases very sharply. This behavior in virtual height may be anticipated qualitatively from the electron density as a function of height (see solid curves in Figure 5).

A comparison of the exact and calculated values of real height as a function of input frequency is shown in Figure 5. In view of the several approximations utilized in the method, the agreement is generally quite good, Model 1 showing slightly better results. It is felt that the less accurate results for Model 2 are due primarily to numerical inaccuracies in the process of integration. In addition, the occurrence of a maximum electron density for Model 2 renders the calculated values of real height very sensitive to small errors in the numerical procedure near the maximum height.

As indicated in Section 5, the accuracy of the method may be improved by the introduction of additional parameters. However, the gain in accuracy will be small while the additional amount of computational labor required will be quite large. The present procedure, utilizing only one parameter, offers a fairly simple method, without the burden of a great deal of numerical work, for determining real height from virtual height data.

7. SUMMARY AND CONCLUSIONS

A method previously developed for the determination of real height from virtual height data has been modified and simplified by representing the entire dispersion curve by a single power law curve with only one parameter. The resulting real height-virtual height relation can now be solved in a simple way for the real height. To test the accuracy of the method, virtual heights were computed for two parabolic models of the ionosphere and the corresponding real height values then obtained by the present method. The results obtained show that the calculated values of real height were in very good agreement with the exact values.

To show the improvement obtainable with the introduction of additional parameters, a two-parameter function, which gives a somewhat more accurate representation of the dispersion curve than does the one-parameter function, has been obtained for one case. However, the amount of computational labor required is considerably greater than with the present method.

In view of its simplicity and accuracy, it is felt that the present one-parameter method is a useful analytic tool for determining real height from ionosonde data.